

## SUPPLEMENTARY INFORMATION

### Inkjet printed mesoscopic perovskite solar cells with custom design capability

Anand Verma<sup>a</sup>, David Martineau<sup>b</sup>, Sina Abdolhosseinzadeh<sup>a,c</sup>, Jakob Heier<sup>a</sup>, Frank Nüesch<sup>a,c</sup>

<sup>a</sup> Laboratory for Functional Polymers, Swiss Federal Laboratories for Materials Science and Technology (Empa), Überlandstrasse 129, CH-8600 Dübendorf, Switzerland.

<sup>b</sup> Solaronix, SA, Rue de l'Ouriette 129, CH-1170 Aubonne, Switzerland

<sup>c</sup> Institut des matériaux, École Polytechnique Fédérale de Lausanne (EPFL), CH-1015 Lausanne, Switzerland.

#### Inkjet printed individual layers:

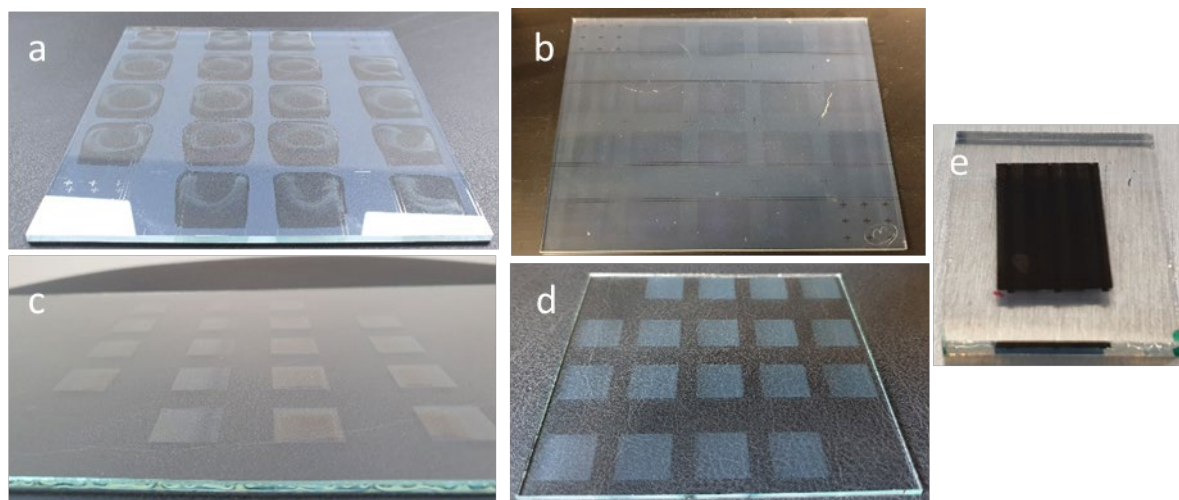


**Fig. S1** Photographs of the inkjet printed c-TiO<sub>2</sub> layer with undesired drying effects (a), c-TiO<sub>2</sub> optimized layer (b), optimized m-TiO<sub>2</sub> (c) and m-ZrO<sub>2</sub> (d), respectively, Individual MPSC with inkjet printed carbon electrode (e).

## **Ink Development**

### **Compact TiO<sub>2</sub>**

Inks were developed from the stock TAA solution consisting of a 75wt% titanium diisopropoxide bis(acetylacetonate) concentrate in isopropanol (iPrOH). The inkjet printing tests were performed with various dilutions of TAA in iPrOH. A PTFE 0.45  $\mu$ L filter was used to filter the inks before de-gassing and de-foaming using rotation of 1000 rpm on Thinky mixture equipment. The dilutions 1:80 vol, 1:60 vol and 1:40 vol/vol yielded poor jetting as well as a very thin film formation. The 1:20 vol/vol yielded an inhomogeneous dried film but mean thickness was  $50 \text{ nm} \pm 10 \text{ nm}$  with two-pass wet on wet printing with a resolution of 1000\*1000 dpi. The inhomogeneity can be explained by poor jetting behavior due to low viscosity (viscosity of iPrOH at 25°C is 1.96 mPa·s) of the ink and drying effects due to fast evaporation (boiling point of iPrOH is 82.6°C). To improve the jetting and wetting as well as drying, we followed the strategy of solvent mixtures of high and low boiling point to counter coffee ring effect induced by Marangoni flow in the thin wet film. We screened various high boiling and low boiling point solvent mixtures like ethylene glycol:iPrOH, tetralin:iPrOH, terpineol:iPrOH, ethylene glycol:ethanol, tetralin:ethanol, terpineol:ethanol. All the solvent mixture showed improved jetting and drying. Terpineol:xylene mixture yielded stable jetting as well as very homogeneous wet and dry film formation (Fig. S1b). The TAA/binary solvent mixture 1:16 vol/vol yielded stable jetting as well as very homogeneous wet and dry film formation (Fig. S1b). The final ink composition has a viscosity of 2.1 mPa·s and surface tension of 23.1 mN/m. It is in the wetting envelope of the FTO substrate, which has a surface free energy of 50.23 mN/m (Table S1, Fig. 2). The ink yielded a homogeneous and pinhole free layer of 60 nm in thickness after firing at 500°C for 1hr. The printing was done in two-pass wet on wet.

### **Mesoporous TiO<sub>2</sub>**

We used a binary solvent mixture of terpineol and iPrOH for dilution of the screen-printing m-TiO<sub>2</sub> paste ink from Solaronix. A dilution of 6 vol m-TiO<sub>2</sub> screen printing

paste in 5:5 vol/vol binary solvent ink yielded stable jetting as shown in Fig. S2. Wetting was also optimal as predicted by the wetting envelope shown in Fig. 2. We observed that filtering of the ink through 1  $\mu\text{m}$  PTFE filter (lower pore sizes were clogged) was better when the dispersion was ultra-sonicated for 15 min. To reach a thick and continuous layer formation, the drops of ink per inch or dots per inch (dpi) was optimized. With drop placement of 200\*200 dpi lead to partial merging of drops on the substrate leading to non-continuous film formation, with 2000\*2000 and 1500\*1500 dpi high spreading beyond c-TiO<sub>2</sub> was observed. With a resolution of 1000\*1000 dpi good pinning of the printed square pattern was observed with single pass. With double pass printing (wet on wet) a little spreading was observed, but the deposited area still remained within the c-TiO<sub>2</sub> layer. The wet films were dried at various temperatures from 50 °C, 70 °C, 90 °C and 110 °C for 10 min and the latter was found to be most optimal with no coffee ring formation. The dried layers were then fired at 500°C for 1 hr on a titania hot plate before receiving m-ZrO<sub>2</sub> layer.

### **Mesoporous ZrO<sub>2</sub>**

The challenge is to formulate a stable nanoparticle dispersion, which should not clog the printhead nozzles as well as have high enough concentration to form a 1000 nm thick layer after firing at 500°C. We followed a similar binary solvent strategy used for m-TiO<sub>2</sub> ink development. Spectra printhead was used for depositing higher ink volumes required to reach the desired thickness. The screen printing paste from Solaronix was diluted with a binary solvent where both the solvents fall in the stable area of wetting as shown in Fig. 3. Series of concentrations and ratio of solvent mixture were screened and the ink with 6 vol of screen printing paste in 5:5 vol/vol of binary solvents gave stable jetting with no satellite formation as well as homogenous layer formation (Fig. S2 and Fig. S1, respectively). The desired thickness was reached with a resolution of 1000\*1000 dpi with two times wet on wet printing. The wet films were dried on a hot plate for 10min at 110°C in ambient condition. The dried films were then fired at 500°C for 1 hr before receiving carbon layer.

## Carbon

Carbon layer was fabricated by screen-printing using the commercially available screen printing paste from Solaronix and the previously reported procedure<sup>24</sup>. The devices were later completed by infiltrating MAPbI<sub>3</sub> precursor ink.

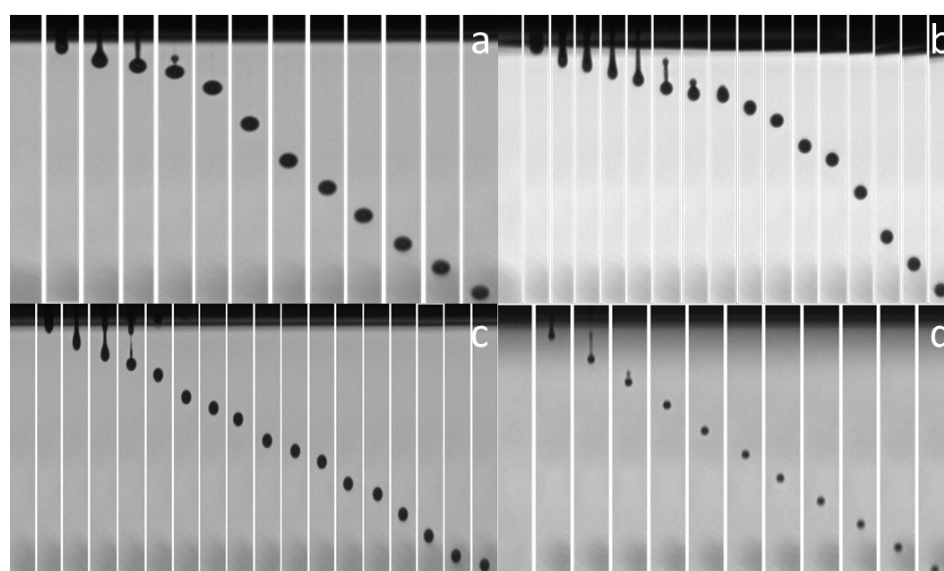
Initial trials to formulate inkjet printable carbon inks were not successful as we tried to reproduce a reported inkjet ink and process<sup>20</sup>. This ink lead to clogging of nozzles and thus rendered unprintable. Super P carbon nanoparticles with 30nm particle size from Alfa Aesar were dispersed in NMP and DMF solvents with 15mg/ml concentration<sup>20</sup> using an ultrasonic probe for 30min in an ice bath to quench solvent evaporation. These inks also yielded poor jetting on Dimatix (10 pl) printhead. We managed to get a thin film of carbon nanoparticle but the wet film de-wetted while drying on a hotplate at 110°C. Solvent mixture approach with NMP:iPrOH (1:1) was investigated but yielded no improved dried film formation. We introduced ethyl cellulose organic binder in the solvent mixture for better adhesion and were able to get stable jetting. The layer formation was acceptable after drying and even after ten printing passes the layer thickness was observed to be very thin. The fully inkjet printed stack was prepared to check the influence of the inkjet printed carbon layer. The high resistance at the carbon electrode yielded a PCE of 0.1%. Metal oxide nanoparticles like ITO, AZO, ATO were also investigated. These metal oxide nanoparticles were introduced into carbon ink to increase the conductivity of the layers. Unfortunately, not much improvement in jetting, clogging and device performance was obtained. The highest PCE achieved was 0.2% with ITO nanoparticles. Thus, a significant effort and development work is still needed. For the infiltration of CH<sub>3</sub>NH<sub>3</sub>PbI<sub>3</sub> (or MAPbI<sub>3</sub>) into the mesoporous stack a Dimatix print-head was used.

**Table S1** Polar and disperse part of the surface energy of solvents being used in the developed inks.

Solvent	Polar component (mN/m)	Disperse component (mN/m)
Tetralin	2	19.6
Xylene	1	17.8
Terpineol	3.6	17.1
Ethanol	8.8	15.8
Isopropanol	6.1	15.8
Ethylene glycol	11	17

**Table S2** Rheological properties of the inks developed for inkjet printing.

ink	Density (g/cm <sup>3</sup> )	Viscosity (mPa.s)	Surface tension (mN/m)
c-TiO <sub>2</sub>	0.8	2.1	23.1
m-TiO <sub>2</sub>	0.9	9.8	24.0
m-ZrO <sub>2</sub>	0.8	9.1	21.9
MAPI	1.13	1.7	33.4

**Fig. S2:** Stable jetting and drop formation as well as the absence of satellite formation is shown by the stroboscope images for c-TiO<sub>2</sub> (a), m-TiO<sub>2</sub> (b), m-ZrO<sub>2</sub> (c) and MAPI (d) inks. The jetted drops are imaged at an interval of 20  $\mu$ s.

### AFM of metal oxide layers:

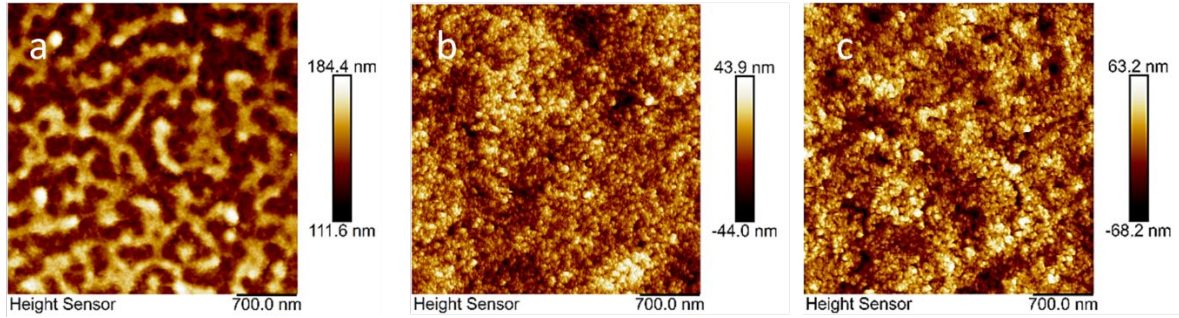


**Fig. S3** AFM images of the three oxide layers of the stack deposited by inkjet printing: c-TiO<sub>2</sub> (a), m-TiO<sub>2</sub> (b) and m-ZrO<sub>2</sub> (c).

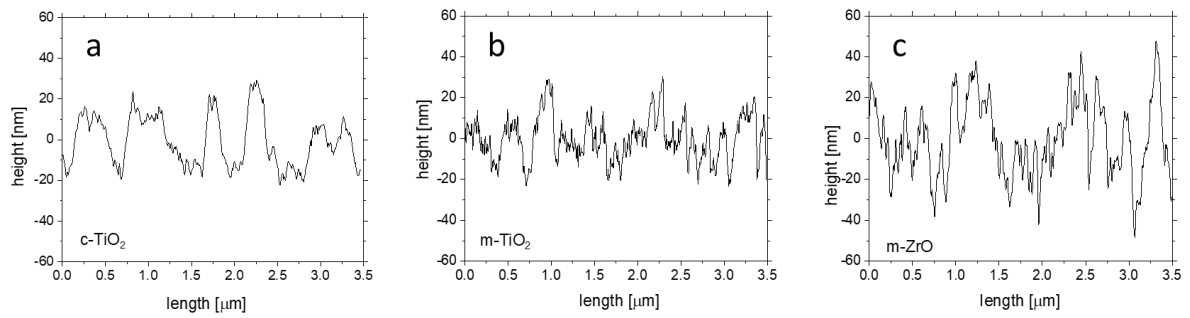


**Fig. S4** Line profiles of the AFM images presented in Fig. S3. The average roughness ( $R_a$ ) and root mean squared roughness ( $R_q$ ) were respectively 12.4 nm and 10.8 nm for c-TiO<sub>2</sub> (a), 11.8 nm and 9.4 nm for m-TiO<sub>2</sub> (b) and 18.4 nm and 14.6 nm for m-ZrO<sub>2</sub> (c).

## X-ray analysis

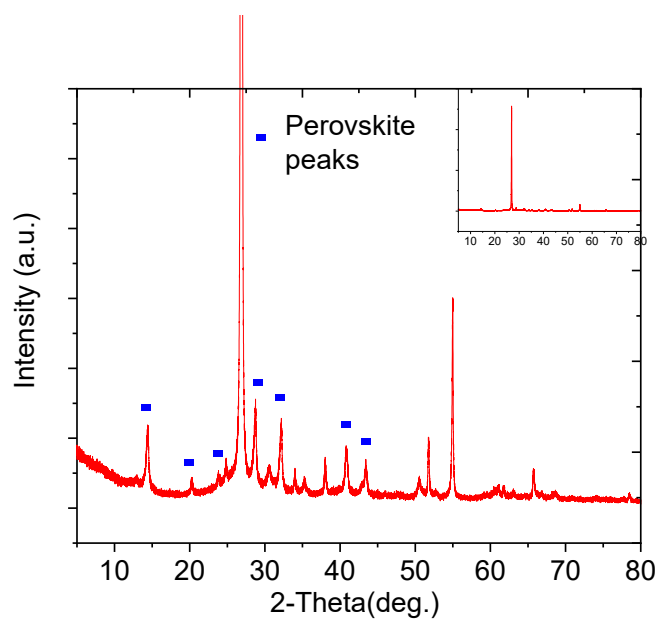


**Fig. S5** X-ray diffraction (XRD) patterns of the inkjet deposited MPSC stack after infiltrating  $\text{CH}_3\text{NH}_3\text{PbI}_3$  (MALI) and annealing. The dominating (101) reflection at  $2\Theta=25.3^\circ$  is attributed to anatase  $\text{TiO}_2$  (inset). At reduced intensity scale, the characteristic reflections of the cubic phase of the MALI perovskite crystal are clearly visible (blue squares). The absence of a reflection peak at  $2\Theta = 12.5^\circ$  reveals that all the precursor ink has been transformed to the organo metal halide perovskite and that no undesirable  $\text{PbI}_2$  is present.

## MAPbI<sub>3</sub> optimization

**Table S3** The table shows the influence of amount of perovskite precursor filling in the mesoporous structure and influence of substrate temperature.

Number of passes	Ink Volume (μL)	Substrate temperature(°C)	PCE (%) Reverse	PCE (%) Forward	PCE (%) Mean
1x	1,5	25	1.4	1.4	1.4
2x	3	25	13.1	11.5	12.3
3x	4.5	25	13.1	12	12.5
1x	6	25	8.8	7.3	8

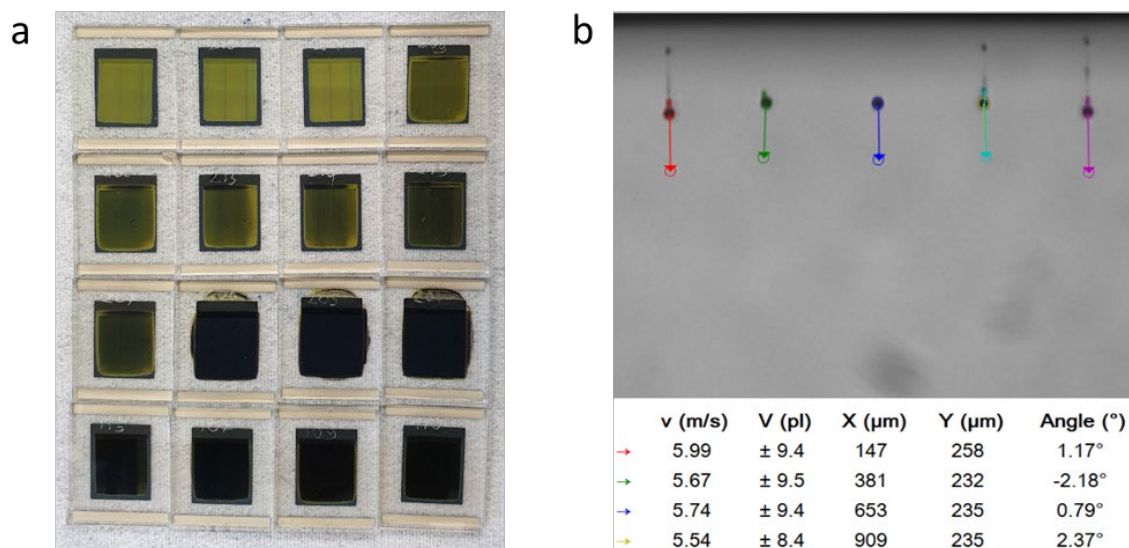
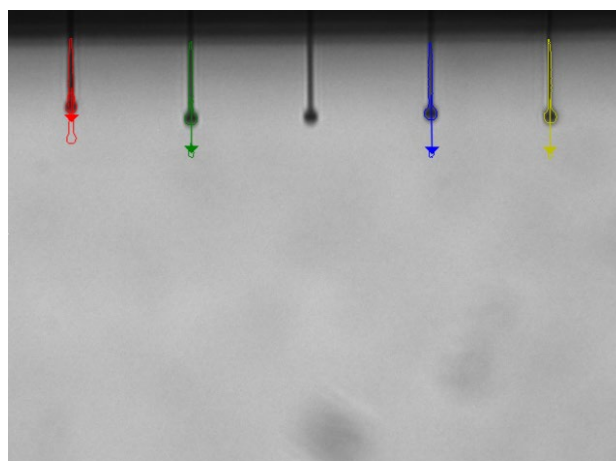


**Fig. S6** Effect of ageing on the degree of MAPbI<sub>3</sub> filling of full MPSC stacks using inkjet infiltration. Devices were aged for 3 months and were photographed from the FTO glass side; yellow (top left) represents partial filling to black (bottom-right) fully filled cells (a). Drop volume and drop velocity of MAPbI<sub>3</sub> perovskite precursor solution using dimatix 1 pL drop volume printhead (b).



## Inkjet printing carbon layer

The developed carbon ink was printed on all oxides inkjet printed layers. Jetting of the ink was possible but clogging could not be avoided with time. The inks were filtered using 1  $\mu\text{m}$  pore size filter before filling into the Dimatix cartridge.



	$v$ (m/s)	$V$ (pL)	$X$ ( $\mu\text{m}$ )	$Y$ ( $\mu\text{m}$ )	Angle ( $^\circ$ )
→	2.90	$\pm 15.1$	135	176	$0.44^\circ$
→	4.70	$\pm 18.0$	388	198	$0.57^\circ$
→	4.93	$\pm 16.0$	894	194	$0.93^\circ$
→	4.65	$\pm 14.0$	1146	202	$0.16^\circ$

**Fig. S7:** Drop volume and drop velocity of carbon ink in NMP:iPrOH using dimatix 10 pL drop volume printhead. Satellite formation can be observed in the jetting image.

## Carbon and metal oxide inkjet printing

**Table S4** Photovoltaic parameters of inkjet printed carbon and ITO cells.

Inkjet printed layer	$V_{oc}$ (V)	$J_{sc}$ ( $\text{mA}/\text{cm}^2$ )	FF (%)	PCE (%)
Carbon	0.78	0.1	25.5	0.02 (0.1 At $V=0.5\text{V}$ )
ITO	0.87	0.9	27.6	0.2